Fluid Phase Equilibria 461 (2018) 8–14

Contents lists available at ScienceDirect

Fluid Phase Equilibria

journal homepage: www.elsevier.com/locate/fluid

Liquid–liquid equilibrium compositions and global phase behavior for the lignin–acetic acid–water system at 70 and 95 °C

Junhuan Ding, Adam S. Klett, Jordan A. Gamble, Graham W. Tindall, Mark C. Thies*

Department of Chemical and Biomolecular Engineering, Clemson University, Clemson, SC, 29634, USA

ARTICLE INFO

Article history:
Received 5 October 2017
Received in revised form
3 January 2018
Accepted 5 January 2018
Available online 10 January 2018

Keywords:
Lignin
Acetic acid
Liquid–liquid
ALPHA
Phase behavior

ABSTRACT

Liquid–liquid equilibrium (LLE) compositions were measured for the pseudoternary system lignin –acetic acid–water at 70 and 95 °C, conditions of interest for the Aqueous Lignin Purification using Hot Acids (ALPHA) process for the purification and fractionation of lignin. Other regions of phase behavior, including a narrow region of LLE at high acetic acid (AcOH) concentrations, as well as solid–liquid (SL) and solid–liquid–liquid (SLL) equilibria, were also identified so that the global phase behavior could be mapped out. For both temperatures, tie-lines encompassing the entire region of "ALPHA" LLE were measured, from near the liquid–liquid critical point in the AcOH-rich region to the solid–liquid–liquid (SLL) phase boundary in the water-rich region. This LLE region exhibited several interesting characteristics. Surprisingly, there was essentially no difference between the solvent compositions in the solvent-rich vs. the lignin (polymer)-rich phase, indicating that the solvent mixture is exhibiting the properties of a single liquid solvent with respect to the lignin polymer. Furthermore, a strong maximum was measured on the lignin-rich side of the binodal curve, which can occur when a solvent mixture consists of strongly associating fluids. The average molecular weight of the lignin in the lignin-rich phase was found to be an order-of-magnitude higher than in the solvent-rich phase. Acid-catalyzed lignin condensation reactions were found to occur at the highest AcOH concentrations and temperatures in the lignin-rich phase, but there was no impact on the measured phase compositions.

1. Introduction

Lignin, a biopolymer found in plants and woody biomass (see Fig. 1), is the only abundant, biorenewable polymer with aromaticity. Thus, it is attracting increased interest, both for the catalytic depolymerization of lignin into platform (e.g., BTX) chemicals [1,2] and for the valorization of lignin into precursors suitable for materials applications, such as phenol–formaldehyde resins [3,4] and polyurethane foams [5,6]. A large source (~50 million tons/yr [7]) of lignin is the pulp-and-paper industry, which the Kraft pulping process dominates [8]. Here it is separated from cellulose during digestion and recovered in an intermediate stream known as black liquor. Although today this black liquor is primarily burned for its heating value, several commercial processes for recovering "Kraft" lignin as a low-ash biomaterial/polymer have recently come on-line (i.e., LignoBoost [9] and LignoForce [10]), and another (SLRP [11]) is in the final stages of development before commercialization.

Lignin is like any other polymer in that its separation into fractions of controlled molecular weight can be an important part of its development for specific applications [12,13]. Furthermore, for many applications the polymer needs to be devoid of metals contamination, which can poison catalysts used for downstream processing [14] or have a deleterious effect on materials properties [15–17]. The Aqueous Lignin Purification with Hot Acids (ALPHA) process [18,19] was developed to address both of these issues in a sustainable manner. In brief, the ALPHA process consists of contacting low-ash Kraft lignin with hot acetic acid (AcOH)–water mixtures such that two liquid phases are formed, one solvent-rich and one lignin (polymer)-rich. Here, "solvent-rich" refers to the phase whose composition is richer in solvent, and "lignin-rich" refers to the phase whose composition is richer in the polymer, which here is lignin. The solvent phase has a high selectivity for the metals, with about an order-of-magnitude reduction in metals content being obtained for each equilibrium stage employed. Furthermore, the lignin partitions between the two phases according to molecular weight (MW), with the solvent-rich phase containing the lower MW and the lignin-rich phase the higher MW

* Corresponding author.
E-mail address: mcths@clemson.edu (M.C. Thies).

https://doi.org/10.1016/j.fluid.2018.01.002
0378-3812/

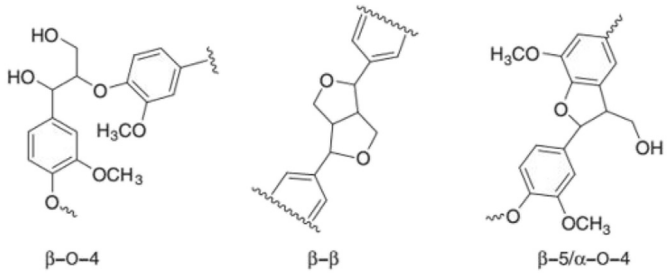

Fig. 1. Representative structures comprising the biopolymer lignin.

portion of the lignin [18]. Thus, purification and fractionation of the lignin take place simultaneously. In addition, by varying the AcOH/H_2O ratio of the feed solvent over a wide range (e.g., 70/30 to 30/70), the lignin can be distributed almost completely into one phase or the other – or it can be split between the two phases in a desired ratio. Low-MW, ultrapure lignin would be desirable for coatings applications [20,21] and high-MW, ultrapure lignins as precursors for carbon fibers [22,23]. In fact, recent results [13] indicate that ALPHA can be used to generate fractions suitable for such applications by varying the processing conditions.

Although the effectiveness of ALPHA in removing metals from lignin and in generating ultrapure lignins of a specified molecular weight has been reported [18,24], the region of liquid–liquid equilibrium (LLE) where ALPHA is practiced has yet to be investigated. No phase compositions or tie-lines have been measured, and the other regions of phase behavior for the pseudoternary lignin–acetic acid–water system have yet to be determined.

Previous, related work is scarce. Our group [25] used both EIS and visual observation to determine the temperature at which lignin liquefied in the presence of AcOH/H_2O mixtures to form LLE, but no phase compositions were measured. Sixta and co-workers [26] measured both LLE and the other regions of phase behavior for the pseudoternary system lignin–γ-valerolactone–water at ambient temperatures; however, the LLE compositions and phase boundaries were difficult to determine because of the presence of emulsions and lignin agglomerates. Yang and Rasmuson [27,28] measured LLE and mapped out the five different regions of phase behavior for the ternary system butyl paraben–ethanol–water at ambient temperatures (butyl paraben is structurally similar to the lignin monomer *p*-coumaryl alcohol).

In this work, LLE tie-line compositions for the lignin–acetic acid–water system were measured at 70 and 95 °C; in addition, the other regions of phase behavior were identified, enabling the construction of pseudoternary phase diagrams for this system. The molecular weight of the lignin in each of the liquid phases was also determined.

2. Materials and methods

2.1. Materials

A low-ash Kraft lignin was isolated from a softwood black liquor using the lignin-recovery process known as SLRP [11,29,30]. The black liquor had a Kappa number of 25 and a solids content of 42 wt %. "SLRP" lignin is similar to low-ash Kraft lignins produced by Domtar (i.e., BioChoice) and Ingevity (Indulin AT), which are also recovered from Kraft black liquor via acidification/precipitation processes. Lignin organic purity was determined to be 99% via a simplified version of the Klason method [31], and the inorganic content of 1% ash was determined by combustion. The lignin was dried in a vacuum oven at ambient temperatures and 10 mm Hg for 24 h from its original water content of 30–40 wt % down to 5–9 wt % (as determined by Karl Fischer titration, see below) and then stored in a desiccator for use in the phase-behavior experiments described below. Glacial acetic acid, ACS grade, 99.7% purity (cat. no. MKV193-45), and anhydrous pyridine, 99.8% purity by GC (cat. no. 270970), were supplied by VWR. Hydranal® Solvent (cat. no. 34800) and Hydranal® Titrant 5 (cat. no. 34801) for volumetric, two-component Karl Fischer titration were supplied from Sigma Aldrich. Lithium bromide (cat. no. 35705–14) and HPLC-grade (99.7+%) N,N-dimethylformamide (cat. no. AA22915-K7) for GPC analysis were obtained from VWR. Deionized water (resistivity of 18.2 MΩ cm) was obtained from an in-house distillation apparatus followed by a water purification unit (Millipore Milli-Q Academic).

2.2. Phase-behavior measurements

Phase-behavior measurements for lignin–acetic acid–water were carried out in 9.5-dram glass vials (VWR part no. 66012–066) that were typically charged with a sample consisting of ~1.5 g of lignin (from the desiccator) and ~13.5 g of the solvent mixture. A magnetic stirring bar of appropriate size (Fisher, Part No. 14-512-121, 9.5 mm i.d. x 10 mm long) was then added to the vial to facilitate mixing and the approach to equilibrium, and the vials were sealed with PTFE/silicone septum caps (VWR part no. 89042–292). A 1-mm o.d., grounded, T-type thermocouple (Omega part no. SCPSS-040G-6-SHX) was inserted through the septum cap and used to monitor the temperature of the contents of the vial. (The thermocouple was previously calibrated against a secondary standard RTD (Burns Engineering, Model No. 18072-A-6-30-0-A/LT60) to an accuracy of ±0.1 °C.) The temperature of the vial and contents was maintained with a magnetically stirred, insulated, 2-L silicone oil bath, heated with a 200-W quartz immersion heater (VWR part no. 470122–464) and temperature-controlled with an OMEGA Series CN8500 controller. Temperature oscillations in the bath averaged less than 0.2 °C from the desired set point. The vial containing the sample was clamped into the oil bath such that the vial contents were always immersed below the level of the oil bath.

For a typical experiment, the vial and its contents were immersed into the bath and stirred at a rate of 350 rpm, reaching the temperature set point in ~7 min; henceforth, temperature oscillations within the vial did not exceed ±0.2 °C. During this time, the system would pass through the solid–liquid phase-transition temperature for the lignin–acetic acid–water system [18]; thus, the solid lignin particles would liquefy in the presence of the solvent mixture, first forming swollen particles and then completely liquefying to form liquid droplets that would rapidly coalesce (i.e., within 5 s) to form the second, lignin-rich liquid phase at the bottom of the vial. A total of 30 min from the initial immersion time at temperature was allowed for equilibration of the two liquid phases.

The solvent-rich and lignin-rich phases were then prepared for composition analysis. In particular, the vial was removed from the bath, and the solvent-rich phase was decanted off into another vial. Both vials were then capped, allowed to cool, and weighed. As the samples cooled, solid lignin precipitated from the solvent-rich phase, and the lignin-rich phase solidified. The samples were then homogenized by the addition of ~10 g of pyridine to each vial, effecting complete dissolution of the lignin and resulting in a single liquid phase in each vial.

2.3. Determination of phase compositions

The water content of both the solvent-rich and the lignin-rich phases was determined by volumetric, two-component Karl Fischer titration, using a Mettler Toledo model DL31 volumetric KF Titrator. Typically, an aliquot consisting of 0.1 g of homogenized

solvent-rich phase or of 0.3 g of homogenized lignin-rich phase was injected into the titration vessel for analysis. Samples were titrated in triplicate, and water compositions for a given sample were reproducible on average to an error deviation of 1%. The uncertainty in water content was estimated by analyzing an Apura® 1 wt% water standard and was found to be <1% relative error.

To determine the lignin content of the homogenized, lignin-rich phase, 3-mL aliquots of this phase were diluted with 40 mL of DI water in a 50-mL centrifuge vial. This caused the precipitation of the lignin, which was then recovered by centrifugation at 6000 rpm for 30 min. The recovered wet lignin was then dried in a vacuum oven (operating at 10 mm Hg and 50 °C) for 6 h, and the dried mass was taken as the mass of lignin in the aliquot. To determine the lignin content of the solvent-rich phase, vials containing the homogenized, solvent-rich phase were first placed in an oven at 1 atm and 120 °C for ~12 h to evaporate most of the solvent; the remaining solvent was then removed by drying in a vacuum oven at 120 °C and 10 mm Hg for 4 h. The dried lignin solid was then immediately placed in a desiccator (to prevent water absorption) to cool before being weighed. The uncertainty in lignin content (5% for both the lignin-rich and solvent-rich phases) was estimated by measuring out known quantities of lignin, acetic acid, and water in similar ratios to those of actual samples, and analyzing for the lignin in each phase via the methods described above. Finally, the acetic acid content in each phase was determined by difference.

2.4. Molecular weight analysis by gel permeation chromatography (GPC)

The molecular weight of the lignin in each phase was determined by GPC (Alliance GPCV 2000). Two columns were used in series: a Waters Styragel® HT5 column (10 μm, 4.6 mm × 300 mm) followed by an Agilent PolarGel-L column (8 μm, 7.5 mm × 300 mm). The mobile phase consisted of 0.05 M lithium bromide in N,N-dimethylformamide at a flow rate of 1 mL/min. Homogenized samples of each phase were dissolved in the mobile phase at a concentration of 1 mg/mL and filtered using a 0.2-μm nylon-membrane syringe filter (VWR, part no 28145–487). Poly(ethylene glycol) (PEG) calibration standards were used for molecular weight determination and were detected by refractive index using a Waters differential refractometer, while lignin samples were detected by UV–vis with a Waters 2487 detector at 280 nm.

3. Results and discussion

The phase behavior for the lignin–acetic acid–water system is best illustrated as a (pseudo)ternary phase diagram, in which lignin serves as one of the apexes (we use the term pseudoternary because the lignin is not a single component but is polydisperse). Two such diagrams were generated from measurements at 70 and 95 °C and are shown as Figs. 2 and 3. The temperatures selected for measurement are representative of those where ALPHA has been carried out [18,24]. By combining the LLE measurements described in Section 2.2 with the more qualitative observations described below, the various regions of phase behavior that exist for this system have been mapped out and identified. However, as seen in the figures, equilibrium tie-line compositions were obtained only for the liquid–liquid (LL) region where the ALPHA process can be practiced, and for the acetic acid–lignin LL binary located on the left-hand side of the diagram.

The solid–liquid (SL) region on the water-rich side (i.e., right-hand side (rhs)) of each phase diagram was observed by mixing lignin with high-water (e.g., 15/85 AcOH/H_2O) solutions, following the procedure described in Section 2.2. In this region, no phase transition (i.e., liquefaction of the lignin) was observed. A

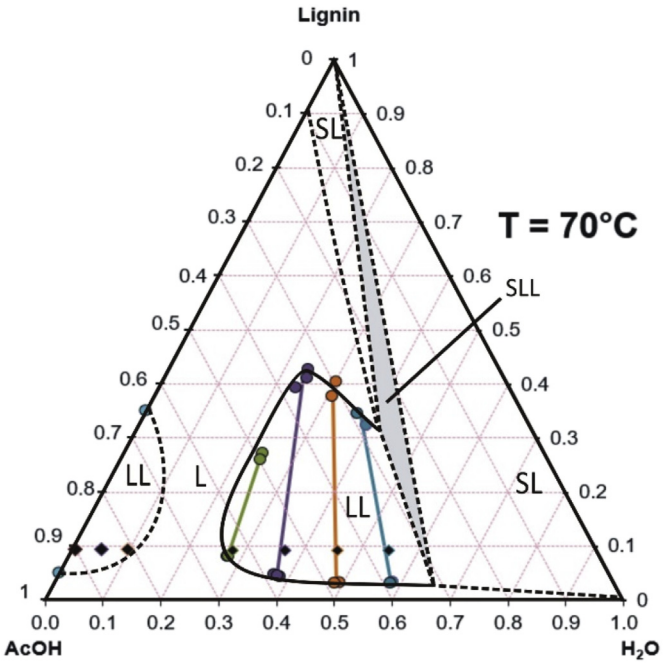

Fig. 2. Pseudo-ternary phase diagram for the lignin–acetic acid–water system at 70 °C and a solvent-to-lignin (S/L) ratio of 9.9:1. Circles (●) are phase compositions and diamonds (◆) are feed compositions.

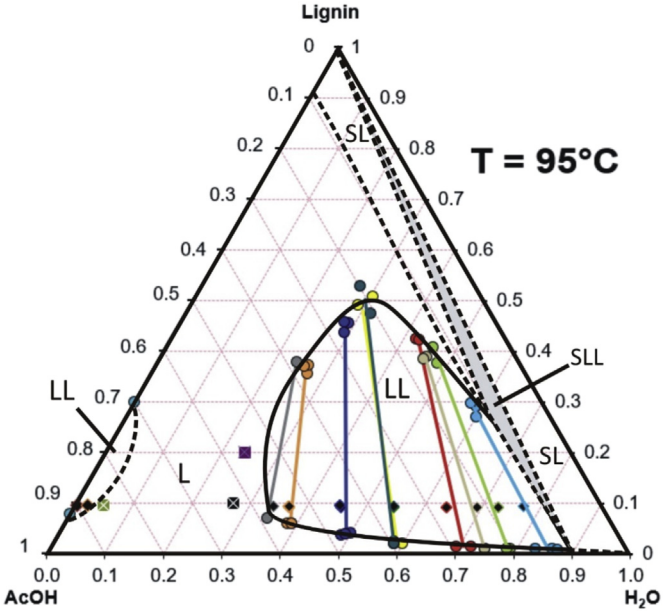

Fig. 3. Pseudo-ternary phase diagram for the lignin–acetic acid–water system at 95 °C and a S/L ratio of 9.8:1. Circles (●) are phase compositions, diamonds (◆) are feed compositions, and squares (■) are measured compositions in the single-phase region.

liquid–liquid (LL) phase split on the left-hand (i.e., AcOH-rich) side (lhs) was observed when lignin was combined with 95/5 and 99.5/0.5 AcOH/H_2O solutions at 70 °C, and with 98/2 and 99.5/0.5 solutions at 95 °C. (Here, the lignin-rich phase is much more viscous (i.e., taffy-like) than the honey-like, lignin-rich phase in the LL region where ALPHA is applied.) However, at slightly higher water concentrations (i.e., 86/14 AcOH/H_2O at 70° and 95/5 AcOH/H_2O at 95 °C), the lignin completely dissolved in the solution to form a single liquid phase, as depicted by the LL phase boundary.

The phase transition from SL to SLL to LLE has previously been measured both visually and by electrochemical impedance spectroscopy (EIS) [25]. These earlier measurements were made at fixed overall lignin–acetic acid–water compositions, with the temperature being increased until the phase transition occurred, see Fig. 4. Referring back to Figs. 2 and 3, one can see how the three-phase, SLL region (and thus the phase transition) "moves" from left to right on the diagram as the temperature is increased from 70 to 95 °C. Because the SLL regions are narrow and the rate of temperature change in the experiments was 1–2 °C/min, only the phase transition from SL to LL was actually observed. The AcOH-rich, SL region near the lignin apex was not actually observed, but is the simplest phase behavior that can exist consistent with the Gibbs phase rule. SL phase behavior is commonly observed in this region for systems where one component is a solid [27].

The tie-line compositions measured in this work were used to define the phase boundary of the LL region where ALPHA can be applied. At 70 °C (Fig. 2), SLE was obtained for 30/70 AcOH/H_2O solutions, bounding the rhs of the LLE region. Analogously, 10/90 AcOH/H_2O gave SLE for the rhs at 95 °C (Fig. 3). Note that these SLE to LLE phase-transition results are in agreement with the above results of Fig. 4. The lhs of the LLE region on both diagrams was bounded by increasing the AcOH/H_2O ratio in the solvent in ~5 wt % increments until one L phase was obtained, but no LL critical point was actually observed. As would be expected, this plait point (and the L region) moves to higher water concentrations with increasing temperature, as is characteristic of upper critical solution temperature (UCST) behavior.

With respect to the tie-line measurements in the LL "ALPHA" region, triplicate experiments were run for each tie line, except that six runs were made for the 40/60 AcOH/H_2O tie line at 95 °C. All of the measured phase compositions are plotted (many overlap, so all cannot be seen), and the tie lines connect the (unplotted) average of all measured phase compositions. The solvent-to-lignin (S/L) ratio was held constant at 9.8 ± 0.2. However, as shown in Fig. 5, the effect of higher (19.9 ± 0.1) and lower (6.2 ± 0.1) S/L ratios on tie-line behavior was also evaluated, with a shift towards the lignin apex with increasing lignin content being observed. Average phase compositions, feed solvent compositions, and S/L ratios for each tie line are tabulated in Table 1. Based on an error analysis

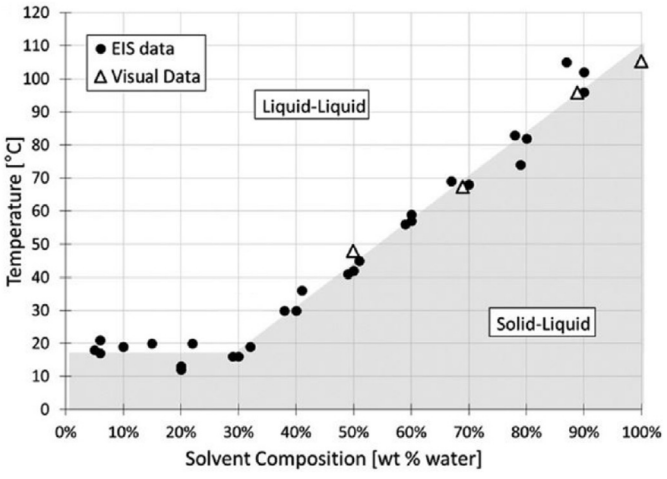

Fig. 4. Temperature vs. composition phase diagram for the lignin–acetic acid–water system, showing phase-transition measurements at the phase boundary between the SL and LL regions. The dark circles (●) represent EIS data, and white triangles (Δ) are from visual observation.
Published by RSC: Reprinted with permission from ref 25. Copyright 2016 Royal Society of Chemistry.

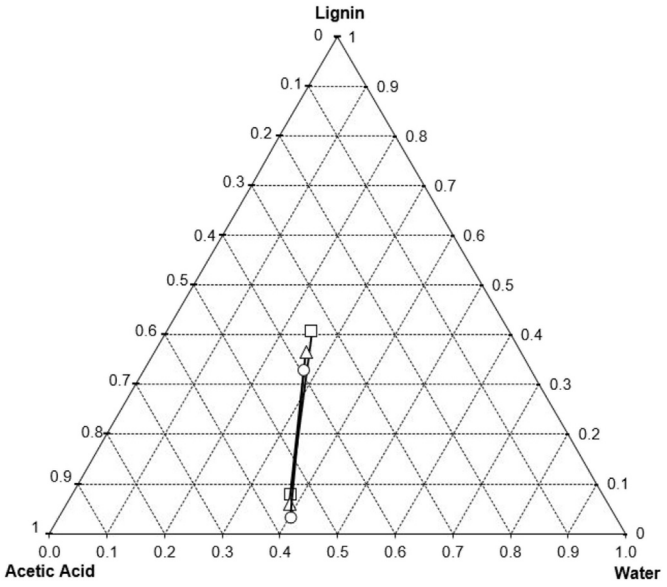

Fig. 5. Measured liquid–liquid equilibrium tie lines for the lignin–acetic acid–water system at 95 °C for a feed composition of 60/40 AcOH/H_2O at S/L ratios of 6.2 (○), 9.8 (Δ), and 19.9 (□).

incorporating the uncertainties in mass-balance closure, component compositions, and temperatures, phase compositions are estimated to be accurate to within 10% relative error for the minor components in the lignin-rich phase and to within 5% relative error for the minor components in the solvent-rich phase.

The LL region of interest (i.e., where ALPHA is practiced) exhibits several interesting characteristics. First, note that there is little selectivity for the partitioning of acetic acid vs. water between the lignin-rich and solvent-rich phases, with $\beta_{AcOH\text{-}H2O}$ for the tie lines at 70 and 95 °C always being close to 1.0 (i.e., monotonically increasing from 0.81 on the lhs to 1.32 on the rhs of the LL region). Given the ability of glacial acetic acid to dissolve a significant portion (i.e., ~50 wt %) of the lignin at ambient temperatures and the inability of water to dissolve lignin, we expected that the AcOH/H_2O ratio in the lignin-rich phase would be significantly higher than in the solvent-rich phase; instead, the feed line and the tie lines are essentially parallel (see Figs. 2 and 3). It is instructive to note that for the model ternary system polymer (3)–solvent (2)–nonsolvent (1) (analogous to lignin–acetic acid–water), the Flory–Huggins (F–H) equation predicts [32] parallel feed and tie lines when the nonsolvent–polymer and solvent–polymer interactions are identical (i.e., $\chi_{13} = \chi_{23}$) and when the solvent–nonsolvent interactions χ_{12} are equal to zero (the latter is the case for an ideal solution). According to Flory, in this situation the mixed solvent is behaving as a single solvent and the "single-liquid approximation" applies. From our perspective, then, one could say that AcOH–-water mixtures form a "new" single solvent that performs much better than either solvent alone – thus, the success of the ALPHA process.

Another interesting feature of our phase diagrams is the prominent maximum on the lignin-rich side of the binodal curve at both temperatures. This behavior can also be predicted with F-H theory, but now by having the nonsolvent–solvent parameter χ_{12} take on negative values (instead of zero as above), indicating a high degree of affinity between the two components, with the sharpness of the maximum increasing as χ_{12} becomes more negative [33].

The mass distribution of lignin between the lignin-rich and solvent-rich phases at both 70 and 95 °C as a function of the feed solvent composition (see Fig. 6) was calculated from knowing the

Table 1
Measured liquid–liquid equilibrium tie lines (in wt %) for the lignin–acetic acid (AcOH)–water system at 70 and 95 °C. Feed Parameters: The solvent composition is given in wt %; S/L Ratio ≡ Solvent-to-Lignin Mass Ratio.

Temp.	Tieline	Feed Parameters		Lignin-Rich phase			Solvent-Rich phase		
		Solvent Composition	S/L Ratio	Lignin	Water	AcOH	Lignin	Water	AcOH
	#	AcOH:H_2O	[g:g]	[%]	[%]	[%]	[%]	[%]	[%]
95 °C	1	15:85	9.62:1	28.65 ± 1.42	58.95 ± 1.14	12.40 ± 0.58	0.93 ± 0.10	85.43 ± 1.94	13.64 ± 1.90
	2	20:80	9.80:1	41.07 ± 3.35	45.69 ± 2.37	13.24 ± 0.99	0.96 ± 0.02	78.58 ± 0.27	20.46 ± 0.29
	3	25:75	9.84:1	38.75 ± 0.35	45.45 ± 0.14	15.80 ± 0.49	1.10 ± 0.04	74.40 ± 0.04	24.50 ± 1.63
	4	30:70	9.89:1	42.46 ± 0.09	42.79 ± 0.43	14.75 ± 0.33	1.35 ± 0.01	71.08 ± 1.72	27.57 ± 1.72
	5	40:60	9.82:1	50.16 ± 2.32	29.83 ± 2.06	20.01 ± 1.44	2.19 ± 0.14	58.83 ± 0.90	38.98 ± 0.84
	6	50:50	9.93:1	45.06 ± 1.11	29.33 ± 0.49	25.61 ± 0.84	3.97 ± 0.22	49.53 ± 0.67	46.50 ± 0.88
	7	60:40	9.75:1	37.00 ± 0.75	26.43 ± 0.94	36.58 ± 0.57	6.65 ± 0.71	38.09 ± 1.00	55.25 ± 0.55
	8	63:37	9.88:1	39.36 ± 0.84	25.09 ± 2.21	35.55 ± 1.98	7.48 ± 0.46	33.66 ± 0.84	58.87 ± 1.30
	9	60:40	19.91:1	34.33 ± 2.30	32.83 ± 2.53	32.84 ± 0.23	3.32 ± 0.01	38.58 ± 0.46	58.10 ± 0.45
	10	60:40	6.20:1	40.64 ± 0.71	25.20 ± 0.50	34.15 ± 0.81	7.76 ± 0.25	37.95 ± 0.28	54.29 ± 0.24
70 °C	11	40:60	9.97:1	33.60 ± 1.51	37.88 ± 1.77	28.52 ± 0.26	3.33 ± 0.23	58.09 ± 0.14	38.58 ± 0.37
	12	50:50	9.94:1	38.57 ± 1.54	30.52 ± 0.36	30.91 ± 1.18	3.22 ± 0.01	48.74 ± 0.53	48.04 ± 0.52
	13	60:40	9.96:1	41.17 ± 1.68	24.02 ± 0.54	34.81 ± 1.99	4.66 ± 0.15	37.70 ± 0.61	57.63 ± 0.46
	14	70:30	9.93:1	26.68 ± 0.86	23.94 ± 0.11	49.38 ± 0.75	8.27 ± 0.08	27.43 ± 0.14	64.30 ± 0.22

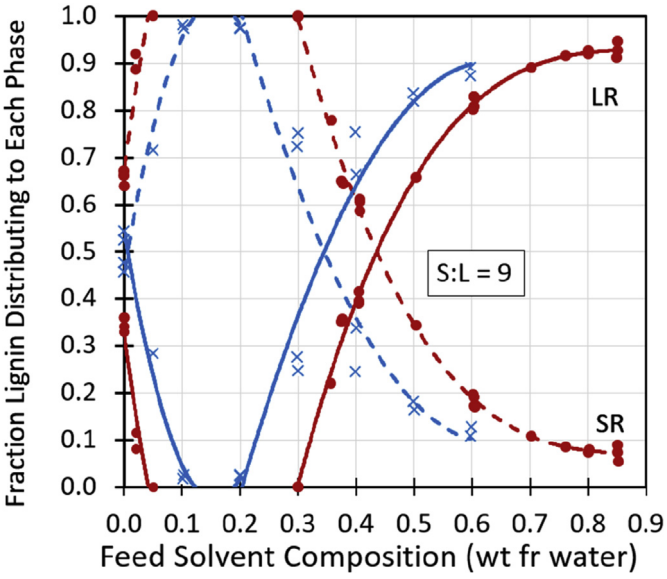

Fig. 6. Mass distribution of lignin between the lignin-rich (LR) and solvent-rich (SR) phases at 70 and 95 °C. Solid lines are for the LR phase and dashed lines are for the SR phase. Circles and red lines represent 95 °C, and crosses and blue lines represent 70 °C. (For interpretation of the references to colour in this figure legend, the reader is referred to the Web version of this article.)

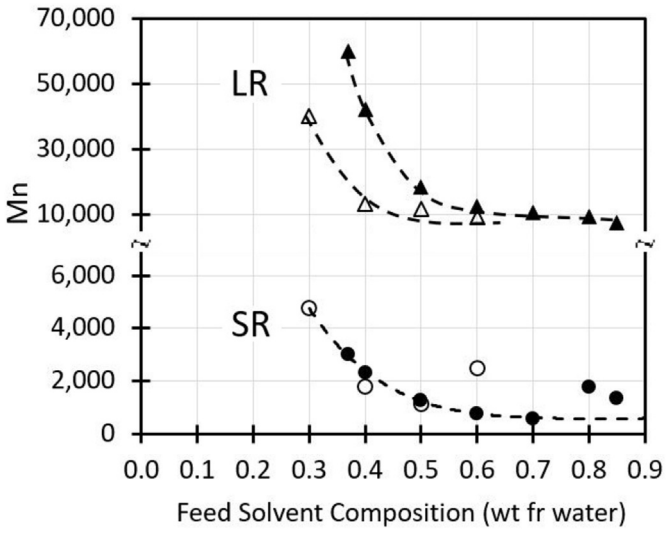

Fig. 7. Molecular weight analysis of lignin in each phase for different feed solvent compositions: number average molecular weight (Mn) of lignin in LR phase at 95 °C (▲) and 70 °C (Δ); Mn of lignin in SR phase at 95 °C (●) and 70 °C (○).

wt % lignin and the total mass of each phase. Moving along the x-axis in solvent composition from pure acetic acid to pure water, we see how the addition of even small amounts of water greatly increases the solvent power, such that >10 wt % water completely dissolves the lignin at 70 °C, forming a single, solvent-rich phase. When the feed solvent contains 20–30% water (with the composition depending on the temperature), the second, lignin-rich phase forms, creating the desired LL phase split where ALPHA can be practiced. As the water content reaches 35–45%, the lignin distributes approximately equally between the two phases; at 65–75% water, only ~10% of the lignin dissolves into the solvent phase.

As shown in Fig. 7, the lignin partitions strongly between the two phases according to molecular weight, with the solvent-rich phase containing the lower MW and the lignin-rich phase the higher MW portion of the lignin. The number average molecular weight (Mn) of the lignin dissolved in the solvent-rich phase (Fig. 7) is generally less than 1000 when the solvent is water-rich, but it monotonically increases with increasing AcOH concentration until at 60/40 AcOH/H_2O, Mn reaches ~2000. At 70/30 AcOH/H_2O and 70 °C, ~70% of the lignin is dissolved in the solvent-rich phase (see Fig. 6), and Mn approaches the feed lignin value of 4900 (Fig. 7). A similar trend of increasing lignin molecular weight with increasing AcOH concentration in the solvent is observed for the lignin-rich phase (Fig. 7), albeit for different reasons: When the solvent is water-rich (e.g., 20 AcOH/80 H_2O), most of the lignin is distributed into the lignin-rich phase, and so Mn for that phase is only slightly larger than that for the feed lignin. But as the AcOH/H_2O concentration increases to 70/30 at 70 °C and 60/40 at 95 °C, the values for Mn (40,000 and 60,000, respectively) are simply too high for what would be expected for simple isolation of the heaviest third of the lignin in the lignin-rich phase (See Fig. 6). Instead, an additional increase in the MW is being caused by the onset of acid-catalyzed condensation reactions, which can occur in the lignin-rich phase at higher AcOH concentrations and temperatures [34,35]. To better quantify this effect, phase-behavior experiments (see Section 2.2) were repeated for a feed solvent composition of 60/40 AcOH/H_2O,

with the total immersion times for the sample vial and its contents being varied from the 30 min that was normally used. Mn of the lignin in each liquid phase are given in Fig. 8 and clearly show how increased residence times in the lignin-rich phase increase molecular weight when the feed solvent is AcOH-rich, particularly at the higher temperatures. For the measurements reported in Table 1, recall (Section 2.2) that 30 min of residence time was chosen as a compromise between the competing effects of allowing adequate time for LLE to be established from the initial solid-liquid mixture vs. the increase in lignin molecular weight that would occur in the lignin-rich phase with increasing time – which itself would affect the LLE of the system. Analysis of the above samples obtained at the different immersion/residence times indicated no measurable impact on equilibrium phase compositions within the previously reported experimental uncertainties.

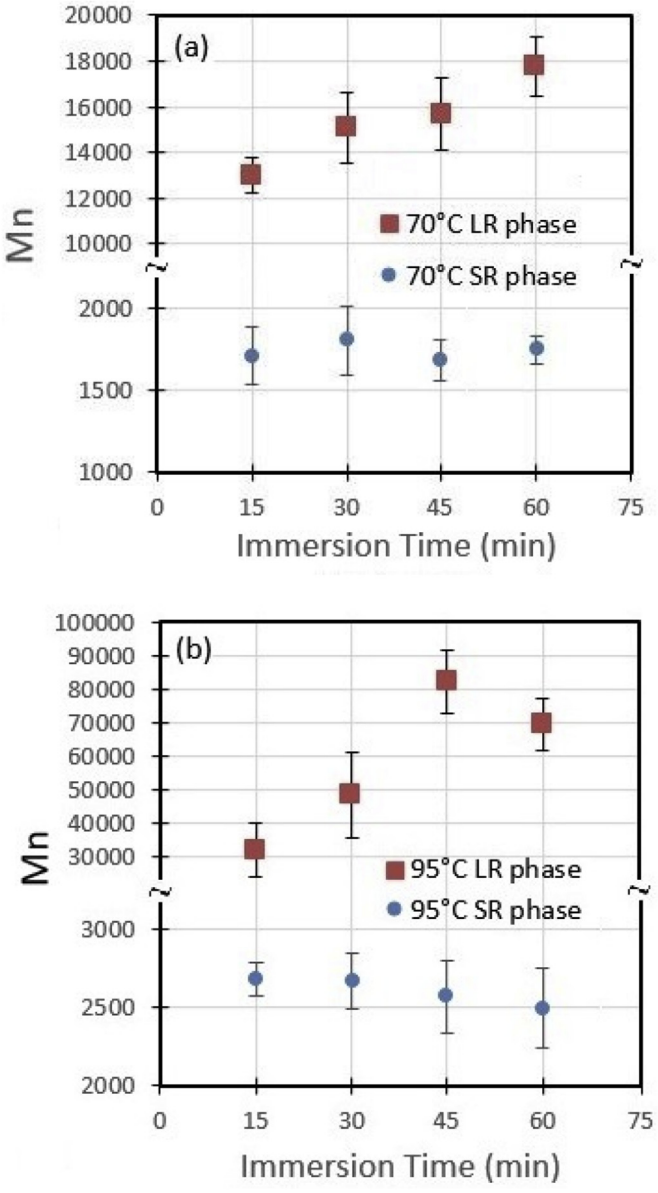

Fig. 8. Changes in Mn for the LR and SR phases vs. residence time at (a) 70 and (b) 95 °C for 60/40 AcOH/H_2O feed composition. For LR phase at 95 °C, the lignin sample at 60 min was only partially soluble in the GPC mobile phase; thus, the reported Mn is too low.

4. Conclusions

Liquid–liquid equilibrium (LLE) phase compositions relevant to the purification and fractionation of lignin via the ALPHA process have been measured for the pseudoternary lignin–acetic acid–-water at 70 and 95 °C. To our knowledge, these are the first LLE phase-composition measurements for lignin dissolved in a solvent or solvent mixture. In addition, the other types of phase behavior present at the above temperatures, including both solid–liquid equilibria and another region of LLE, have been identified, allowing us to place the LLE region of interest for the ALPHA process into its proper context. The phase behavior in the "ALPHA" LLE region is consistent with that of a highly associated solvent mixture (i.e., AcOH/H_2O) acting as a single solvent with respect to the lignin, as there is a strong maximum in the binodal curve, yet having little selectivity of the acetic acid or water to partition between the solvent-rich and polymer-rich phases. The liquid–liquid critical point for the system moves to increasing water concentration with increasing temperature, consistent with UCST behavior. Condensation reactions catalyzed by the acetic acid do occur in the polymer-rich phase, but were found to have minimal impact on the phase compositions for the residence times of 30 min that were employed. Furthermore, when ALPHA is practiced, it is operated in a continuous manner with residence times <30 s, so these types of reactions are essentially eliminated [24]. Finally, the large MW differences (about an order of magnitude) between the lignin that distributes into the solvent-rich vs. the polymer-rich phase indicates the useful of the ALPHA liquid–liquid extraction process for separating lignin into low- and high-MW fractions as required for different applications.

Acknowledgments

This material is based upon work supported by the National Science Foundation under Grant No. CBET-1403873. The authors would also like to acknowledge the Center for Advanced Engineering Fibers and Films at Clemson University for partial financial support. The authors also wish to thank Jed Gist, James Martzin, and Anne Mason for their assistance with the GPC and phase-composition measurements.

References

[1] C. Li, X. Zhao, A. Wang, G.W. Huber, T. Zhang, Catalytic transformation of lignin for the production of chemicals and fuels, Chem. Rev. 115 (21) (2015) 11559–11624.
[2] T.D.H. Bugg, R. Rahmanpour, Enzymatic conversion of lignin into renewable chemicals, Curr. Opin. Chem. Biol. 29 (2015) 10–17.
[3] J.C. Domínguez, M. Oliet, M.V. Alonso, E. Rojo, F. Rodríguez, Structural, thermal and rheological behavior of a bio-based phenolic resin in relation to a commercial resol resin, Ind. Crop. Prod. 42 (2013) 308–314.
[4] W. Qiao, S. Li, G. Guo, S. Han, S. Ren, Y. Ma, Synthesis and characterization of phenol-formaldehyde resin using enzymatic hydrolysis lignin, J. Ind. Eng. Chem. 21 (2015) 1417–1422.
[5] P. Cinelli, I. Anguillesi, A. Lazzeri, Green synthesis of flexible polyurethane foams from liquefied lignin, Eur. Polym. J. 49 (6) (2013) 1174–1184.
[6] J. Bernardini, P. Cinelli, I. Anguillesi, M.B. Coltelli, A. Lazzeri, Flexible polyurethane foams green production employing lignin or oxypropylated lignin, Eur. Polym. J. 64 (2015) 147–156.
[7] R.J.A. Gosselink, E. de Jong, B. Guran, A. Abächerli, Co-ordination network for lignin—standardisation, production and applications adapted to market requirements, Ind. Crop. Prod. 20 (2004) 121.
[8] R. Patt, O. Kordsachia, R. Süttinger, Pulp – Ullmann's Encyclopedia of Industrial Chemistry, 2011.
[9] P. Tomani, The lignoboost process, Cellul. Chem. Technol. 44 (1–3) (2010) 53–58.
[10] L. Kouisni, P. Holt-Hindle, K. Maki, M. Paleologou, The Lignoforce System™: a new process for the production of high-quality lignin from black liquor, J. Fr. 2 (4) (2012) 6–10.
[11] M.A. Lake, J.C. Blackburn. Process for recovering lignin. U.S. Patent 9,260,464, Feb. 16, 2016.

[12] S. Kubo, Y. Uraki, Y. Sano, Preparation of carbon fibers from softwood lignin by atmospheric acetic acid pulping, Carbon 36 (7–8) (1998) 1119–1124.
[13] M.C. Thies, J.-H. Ding, 434b, in: Aqueous Lignin Purification with Hot Acids: Cleaning, Fractionating, and Solvating Lignin for Materials Application, 2017 AIChE Annual Meeting, Minneapolis, MN, Oct 2017.
[14] J.L. McCarthy, A. Islam, Lignin Chemistry, technology, and utilization: a brief history, in: lignin: historical, biological, and materials perspectives, ACS (Am. Chem. Soc.) Symp. Ser. (1999) 2–99.
[15] A.L. Compere, W.L. Grifith, C.F. Leitten Jr., J.T. Shaffer, Low cost carbon fiber from renewable resources, in: A. Falcone, K.M. Nelson, R. Albers (Eds.), International SAMPE Technical Conference Series: Advancing Affordable Materials Technology vol. 22, Soc. Advancement Materials & Process Engineering, Seattle, WA, 2001, pp. 1306–1314.
[16] G. Gellerstedt, E. Sjöholm, I. Brodin, The wood-based biorefinery: a source of carbon fiber? Open Agric. J. 3 (2010) 119–124.
[17] D.A. Baker, T.G. Rials, Recent advances in low-cost carbon fiber manufacture from lignin, J. Appl. Polym. Sci. 130 (2) (2013) 713–728.
[18] A.S. Klett, P.V. Chappell, M.C. Thies, Recovering ultraclean lignins of controlled molecular weight from Kraft black-liquor lignins, Chem. Commun. 51 (2015) 12855–12858.
[19] M.C. Thies, A.S. Klett, D.A. Bruce, Solvent and Recovery Process for Lignin, U.S. Patent Appl. Publ. No. 2016/0137680 A1, May 19, 2016.
[20] J.F. Stanzione, P.A. Giangiulio, J.M. Sadler, J.J. Scala, R.P. Wool, Lignin-based bio-oil mimic as biobased resin for composite applications, ACS Sustain. Chem. Eng. 1 (4) (2013) 419–426.
[21] J.F. Stanzione, J.M. Sadler, J.J. LaScala, R.P. Wool, Lignin model compounds as bio-based reactive diluents for liquid molding resins, Chem. Sus. Chem. 5 (7) (2012) 1291–1297.
[22] H. Mainkaa, O. Tägera, E. Körnera, L. Hilfertb, S. Busseb, F.T. Edelmannb, A.S. Herrmannc, Lignin – an alternative precursor for sustainable and cost-effective automotive carbon fiber, J. Mater. Res. Technol. 4 (3) (2015) 283–296.
[23] M. Zhang, A.A. Ogale, Carbon fibers from dry-spinning of acetylated softwood kraft lignin, Carbon 69 (2014) 626–629.
[24] A.S. Klett, A.M. Payne, M.C. Thies, Continuous-flow process for the purification and fractionation of alkali and organosolv lignins, ACS Sustain. Chem. Eng. 4 (12) (2016) 6689–6694.
[25] A.S. Klett, J.A. Gamble, M.C. Thies, M.E. Roberts, Identifying thermal phase transitions of lignin-solvent mixtures using electrochemical impedance spectroscopy, Green Chem. 18 (2016) 1892.
[26] H. Lê, A. Zaitseva, J.P. Pokki, M. Ståhl, V. Alopaeus, H. Sixta, Solubility of organosolv lignin in γ-valerolactone/water binary mixtures, Chem. Sus. Chem. 9 (20) (2016) 2939–2947.
[27] H. Yang, Å.C. Rasmuson, Phase equilibrium and mechanisms of crystallization in liquid–liquid phase separating system, Fluid Phase Equil. 385 (2015) 120–128.
[28] H. Yang, Å.C. Rasmuson, Investigation of batch cooling crystallization in a liquid–liquid separating system by PAT, Org. Process Res. Dev. 16 (6) (2012) 1212–1224.
[29] J. Velez, M.C. Thies, Solvated liquid-lignin fractions from a Kraft black liquor, Bioresour. Technol. 148 (2014) 586–590.
[30] R.J. Stoklosa, J. Velez, S. Kelkar, C.M. Saffron, M.C. Thies, D.B. Hodge, Correlating lignin structural features to phase partitioning behavior in a novel aqueous fractionation of softwood Kraft black liquor, Green Chem. 15 (10) (2013) 2904–2912.
[31] F. Aldaeus, H. Schweinebarth, P. Torngren, A. Jacobs, Simplified determination of total lignin content in kraft lignin samples and black liquors, Holzforschung 65 (2011) 601–604.
[32] P.J. Flory, Principles of Polymer Chemistry, Cornell University Press, New York, 1967, pp. 548–554.
[33] L. Yilmaz, A.J. McHugh, Analysis of nonsolvent–solvent–polymer phase diagrams and their relevance to membrane formation modeling, J. Appl. Polym. Sci. 31 (4) (1986) 997–1018.
[34] S. Yasuda, N. Ito, Behavior of lignin in organic acid pulping. I. Reaction of arylglycerol-β-aryl ethers with acetic acid, Mokuzai Gakkaishi 33 (9) (1987) 708–715.
[35] Y. Sano, S. Shimamoto, M. Enoki, H. Konno, Fractionation of woody biomass with boiling aqueous acetic acid containing a small amount of mineral acid at atmospheric pressure: reactivity of arylglycerol-β-aryl ethers in lignins with aqueous acetic acid containing H_2SO_4, J. Wood Sci. 44 (1998) 217–221.